C1q/TNF-Related Protein 3 Prevents Diabetic Retinopathy via AMPK Dependent Stabilization of Blood-Retinal Barrier Tight Junctions

Zheyi Yan
Thomas Jefferson University - Center City Campus: Thomas Jefferson University
Chunfang Wang
Thomas Jefferson University - Center City Campus: Thomas Jefferson University
Zhijun Meng
Thomas Jefferson University - Center City Campus: Thomas Jefferson University
Lu Gan
Thomas Jefferson University - Center City Campus: Thomas Jefferson University
Rui Guo
Thomas Jefferson University - Center City Campus: Thomas Jefferson University
Jing Liu
Thomas Jefferson University - Center City Campus: Thomas Jefferson University
Wayne Bond Lau
Thomas Jefferson University - Center City Campus: Thomas Jefferson University
Dina Xie
Thomas Jefferson University - Center City Campus: Thomas Jefferson University
Jianli Zhao
Thomas Jefferson University - Center City Campus: Thomas Jefferson University
Bernard L Lopez
Thomas Jefferson University - Center City Campus: Thomas Jefferson University
Theodore A Christopher
Thomas Jefferson University - Center City Campus: Thomas Jefferson University
Ulhas P. Naik
Thomas Jefferson University - Center City Campus: Thomas Jefferson University
Yajing Wang (yajing.wang@jefferson.edu)
Thomas Jefferson University
Xinliang Ma
Thomas Jefferson University - Center City Campus: Thomas Jefferson University

Original investigation

Keywords: CTRP3, iBRB, Tight junction's protein, Permeability, Diabetic Retinopathy

Posted Date: September 30th, 2021

DOI: https://doi.org/10.21203/rs.3.rs-903036/v1

Version of Record: A version of this preprint was published at Cells on February 23rd, 2022. See the published version at https://doi.org/10.3390/cells11050779.

Abstract

Background

The impairment of the inner blood-retinal barrier (iBRB) increases the pathological development of diabetic retinopathy (DR), a severe complication in diabetic patients. Identifying approaches to preserving iBRB integrity and function is a major challenge in DR. C1q/tumor necrosis factor-related proteins-3 (CTRP3) is a newly discovered adipokine and an important biomarker predicting DR severity. We sought to determine whether and how CTRP3 affects the pathological development of non-proliferative diabetic retinopathy (NPDR).

Methods

To clarify the pathophysiologic progress of the blood-retinal barrier in NPDR and explore its potential mechanism, a mouse type 2 diabetic model of diabetic retinopathy was used. The capillary leakage was assessed by confocal microscope with fluorescent-labeled protein in vivo. Furthermore, the effect of CTRP3 on the inner blood-retinal barrier (iBRB) and its molecular mechanism was clarified.

Results

The results demonstrated that CTRP3 protects iBRB integrity and resists the vascular permeability induced by DR. Mechanistically, the administration of CTRP3 activates AMPK signaling pathway and enhances the expression of Occludin and Claudin-5 (tight junction protein) in vivo and in vitro. Meanwhile, CTRP3 improves the injury of human retinal endothelial cells (HRMECs) induced by high glucose/high lipids (HG/HL) and its protective effects are AMPK dependent.

Conclusions

In summary, we report for the first time that CTRP3 prevents diabetes-induced retinal vascular permeability via stabilizing the tight junctions of the iBRB and AMPK-dependent Occludin/Claudin-5 signaling pathway, thus critically affecting the development of NPDR.

Introduction

Despite improvements in clinical patient care, risk factor identification and public health awareness of diabetes are still lack of well-noted. Large population of diabetes leads to diabetic retinopathy (DR), a problematic complication of diabetes, causing blindness especially in developed countries [1]. Diabetic retinopathy is considered as a microvascular complication of endothelial dysfunction, which is characterized by damage of blood-retinal barrier (BRB), and neovascularization [2]. The BRB is composed of two distinct barriers; the outer BRB, consisting of retinal pigment epithelium and the inner BRB (iBRB),

which is formed by the tight junctions between neighboring retinal capillary endothelial cells, and regulates transportation across retinal capillaries. Importantly, the loss of iBRB occurs in the early stage in diabetes [3] [4] (non-proliferative stage, NPDR) and leads to the development of clinically significant DR [5–7]. Determining the novel targets for NPDR not only help for early DR diagnostics, but is also helpful for formulating preventive strategy against advancing to the late stage.

The C1q/tumor necrosis factor-related proteins (CTRPs) are a newly identified adiponectin paralogs consisting of 15 (CTRP1-CTRP15) subtypes [8]. Recent studies reported that regarding the relationship between CTRPs and diabetes, CTRP3 particularly has been shown to exhibit anti-diabetic, anti-inflammatory [9–11] [12] and metabolic regulatory effects in multiple tissues, including vasculature [13]. Notably, we have recently demonstrated that serum CTRP3 is associated with DR, serving as a novel biomarker for DR severity [12]. However, whether CTRP3 regulates diabetes-induced iBRB dysfunction in NPDR, and how it modulates retinal vascular endothelial cells pathophysiological process have never been previously investigated.

The aims of the current study are: 1) to determine whether CTRP3 modulates the barrier pathophysiological process of iBRB in NPDR, mitigating diabetes-induced retinal vascular permeability, and if so, 2) to determine the responsible mechanisms involved.

Methods

HFD/STZ Type 2 diabetes (T2D)-induced DR animal model

All experiments were performed in adherence to the National Institutes of Health Guidelines on the Use of Laboratory Animals and were approved by the Thomas Jefferson University and Shanxi Medical University Committee on Animal Care. In order to establish Type 2 diabetes (T2D) induced DR model, adult C57BL/6J mice were fed high fat diet containing 60% energy from fat (D12492; Open Source Diets) combined with streptozotocin (STZ) (Sigma Chemical, St. Louis, MO) [14]. The mice were fed HFD for 12 weeks to induce obesity, characterized by abnormal glucose tolerance and insulin resistance. The age-matched nondiabetic mice were fed standard diet (SD-diet). Then, mice were subjected to STZ (50 mg/kg body weight, once) at 12 weeks of HFD [14] followed with 8 more weeks of HFD to establish DR model (Supplemental Figure 1A). In addition, mice fed standard diet as control were given an injection of equivalent volume of citrate buffer. Fasting blood glucose level was examined using a RocheAccu-Chek™ blood glucose monitoring systems at the 12 weeks of HFD. Mice were considered diabetic when blood glucose exceeded 12 mmol/L. The globular form of CTRP3 (gCTRP3, 0.5μg/g/d) or double-distilled water was administered to HFD/STZ-T2D mice and the age-matched non-diabetic mice via peritoneally implanted osmotic pumps during the last 2 weeks of HFD. Meanwhile, to inhibit AMPK activation, 100 μl (20 mg/mL) Compound C (Sigma Chemical, St. Louis, MO, USA) was intraperitoneally injected into diabetic mice daily during the last 2 weeks.

Glucose and Insulin Tolerance Assay

To assess glucose tolerance, mice were intraperitoneally injected with D-glucose (1.5 g/kg) after fasting. The venous blood was collected 30 min before (time 0) and after injection at 0, 15, 30, 60 and 120 min. The blood glucose was measured using a Roche Accu-Chek™ glucose monitoring systems per manufacturer's instruction. To assess insulin tolerance, a single dose of Novolin R regular insulin (0.5unit/kg) was intraperitoneally administered to the mice after fasting for 4 hours with free access to water. The blood glucose level was measured as described above.

Capillary permeability assay in vivo

To observe capillary permeability in vivo, the T2D-DR mice and the age-matched non-diabetic mice were anesthetized. Evans Blue (EB) dye (25 mg/kg, 0.5% in PBS) was injected. After the mice were euthanized, mouse ear tissue was collected with an 8 mm skin punch and fixed in 10% formamide at 56°C for 48 hours. The quantification of Evans blue in the tissues was determined by the optical density assessment on Image J (NIH) [15]. To assess CTRP3's role in ear capillary permeability, gCTRP3 (0.5 μg/g/d) or vehicle was administered via peritoneal implanted ALZET osmotic pumps (Cupertino, CA) for 2 weeks to T2D-DR mice and the age-matched nondiabetic mice.

Retinal capillary leakage assay in vivo

Retinal capillary leakage assay was analyzed by a previously reported methods with modification. [15-18] Briefly, mixture of tetramethylrhodamine isothiocyanate conjugate Concanavalin A (TRITC-ConcanavalinA) (indicating vascularity, 25 μg/g, Cat#C860, Thermo Fisher Scientific, MA) and FITC-dextran (indicating vascular leakage, 50 μg/g, Cat#46945, Sigma-Aldrich, MO) were injected from the superior vena cava. Then, the mice were euthanized in 15 minutes and retina tissues were obtained. The retina were flatly mounted and used for examining the retinal vascular pattern. Images were obtained with a Nikon EclipseE800 confocal microscopy (Nikon). 5 images for each eye (full view) were taken. The mean intensity of TRITC-ConcanavalinA and FITC-dextran was determined by Image J software (NIH).

Cell culture and treatments

Human retinal microvascular endothelial cells (HRMECs) (Cat# cAP-0010, Angio-Proteomie, Boston, MA) were plated on six-well plates and cultured at 37°C in 5% CO_2 incubator. Upon reaching 100% confluence, HRMECs were randomized to receive one of the following treatments: 1) Normal glucose normal lipids (NGNL, 5.5 mM D-glucose/19.5mM L-glucose) receiving vehicle or gCTRP3 (0.3, 1, and 3μg/ml, Cat# 00082-01; Aviscera Bioscience, Santa Clara, CA) for 24 hours; 2) high glucose/high lipids (HGHL, 25 mM D-glucose/250 μM palmitates) [19] receiving vehicle or gCTRP3 treatment (0.3, 1, and 3μg/ml) for 24 hours; 25mM L-glucose plus fatty acid-free BSA was used as an osmotic control [20].

iBRB permeability assay in vitro

The permeability of the endothelial membrane was assessed by passage of FITC-dextran through the HRMEC monolayer [21]. To measure endothelial barrier function in iBRB, in vitro transwell

endothelial permeability assay (Sigma-Aldrich, MA) was performed. Briefly, after HRMEC monolayer was built, culture medium was pre-treated with gCTRP3 (3μg/ml) for 15 minutes, then followed by NGNL/HGHL challenge for 24 hours. FITC-dextran (20 μg/ml) was added to upper chamber for 20 minutes. The fluorescence signal in lower chamber was determined at 450 nm using Bio-Rad 450 microplate reader (Bio-Rad, Hercules, CA).

To investigate continuous real-time monitoring of the HRMEC monolayer migration and cell-cell junctions in vitro, we conducted xCELLigence electrical conductivity assays [22, 23]. HRMECs ($3.0x10^4$ cells) were seeded onto a 16-well E-plate. After equilibration, plates were inserted into the xCELLigence station, and the base-line impedance was measured to ensure that all wells and connections were working within acceptable limits. Cell index curves were determined by the xCELLigence RTCA System (Roche, RTCA DP Station) per manufacturer instruction.

Western blot analysis

HRMECs or tissue were lysed by lysis buffer (Cell Signaling). Total protein (50 μg) was loaded on Bio-Rad 4-20% gel system, transferred to PVDF membrane, immunoblotted with one of the following primary antibodies: Serine473 phosphorylated Akt (Cat#4060, Cell Signaling), total Akt (Cat#4691,Cell Signaling), Threonine172 phosphorylated AMPK (Cat#2535, Cell Signaling), total AMPK (Cat#5832,Cell Signaling), Acetyl-CoA Carboxylase(Cat #3662, Cell Signaling), Phospho-Acetyl-CoA Carboxylase (Cat #11818, Cell Signaling), Claudin-1(Cat#13995, Cell Signaling), zo-1 (Cat#13663, Cell Signaling), Claudin-5 (Cat#35-2500, Thermo-Fisher Scientific), Occludin (Cat#71-1500, Thermo-Fisher Scientific)), and ß-Actin (Cat#SC-4778, Sigma). The secondary antibody was obtained from Cell Signaling Company. The membrane was exposed to Super-Signal Reagent (Pierce, Illinois, USA), and imaged on a Bio-Rad ChemiDoc Touch station (Bio-Rad).

Cellular Immuno-fluorescence staining

Cells were fixed with 1% paraformaldehyde for 10 minutes at room temperature. The cells were incubated with primary antibodies against anti-Claudin5 (Cat#35-2500, Thermo-Fisher Scientific) and Occludin (Cat#71-150, Thermo-Fisher Scientific). After overnight incubation at 4°C, the cells were incubated with fluorescein-labeled secondary antibody. The nuclei were counterstained with 4’,6-diamidino-2-phenylindole (DAPI). Micrographs of all immunostains were acquired by Olympus BX51 Fluorescence Microscope and Olympus DP72 image system. Quantification of fluorescence intensity at the cell boundary was performed with Image J (NIH).

Measurement of serum and retinal globular domain CTRP3 (gCTRP3)

Animal retina and serum were collected and stored at -80°C. Frozen retinas were homogenized, centrifuged for 10 min at 13,000 g at 4°C, and the supernatants were collected. The serum was centrifuged for 15 min at 3,000 g at 4°C and the supernatants were collected. gCTRP3 was measured using a commercial ELISA kit (Cat: SK00082-03-100, Aviscera Bioscience, Santa Clara, CA) per the

manufacturer's instruction. The minimum detectable level of CTRP3 is 16 ng/ml (intra-assay coefficient of variability (CV): 4-6%; interassay CV: 8–10%).

Tube formation assay

To examine the impact of CTRP3 on the tube formation of HRMECs, we used a u-slide angiogenesis system (ibidi). Briefly, the plate was coated with Matrigel (growth factor reduced, BD Biosciences). Upon gel solidification, HRMECs ($1x10^4$ cells) were seeded onto pre-coated Matrigel. Then, gCTRP3 (0.3 μg/ml, 1 μg/ml, and 3μg/ml) was added and then the insert was removed. After overnight incubation, the capillary-like structures of HRMECs were photographed with a microscope and analyzed via Image J software (NIH). For conditioned medium experiments, endothelial cell basal medium was replaced with NG medium or HGHL medium.

Small interfering RNA transfection

HRMECs were transfected by siPORTER siRNA transfection kit (Cat#AM4503, Ambion) per manufacturer's protocol with siRNA duplex against AMPK-α1 and universal negative control (Santa Cruz). Briefly, HRMECs were plated on six-well plates. After HRMECs reached 80% confluence, siRNA was applied to each well (final concentration 50 nM). Protein suppression was evaluated by Western blot 72 hours later.

Statistical Analysis

Data were analyzed with GraphPad Prism-7 statistic software (La Jolla, CA). All values are presented as the mean±SD of independent experiments. For analysis of differences between two groups, the unpaired Student t-test was performed. For multiple groups, one-way ANOVA was conducted across all investigated groups. Tukey post hoc tests confirmed where statistically significant differences existed between groups. P values less than or equal to 0.05 were considered statistically significant.

Results

HFD/STZ-induced T2D increased microvascular permeability

The characteristics of DR were illustrated as supplemental Fig. 1 (sFigure1). Compared to ND-fed mice, HFD-fed mice exhibited a significant increase of body weight (sFig. 1B). Meanwhile, the glucose tolerance and insulin tolerance assay revealed that mice exhibited abnormal glucose tolerance and insulin resistance when animals fed with HFD for 12 weeks (sFig. 1C and 1D). However, no significant difference was observed on body weight between the control-treated and HFD/STZ-induced T2D group at 20 weeks (sFig. 1E). Merged confocal images of the retinal flat mounts showed increased vascular leakage after HFD/STZ treatment, demonstrating that the diabetic retinopathy model had been established (sFig. 1G).

Ear capillary permeability assay showed Evans blue dye extravasation (sFig. 1F), suggesting that ear microvascular permeability is increased in this DR model.

CTRP3 exerted protective effect on capillary leakage and retinal capillary leakage in T2D model

Among CTRPs investigated in diabetic patients with microvascular disease, CTRP3 reduction is most significantly associated with DR[12]. With this supportive evidence, we further explored whether CTRP3 plays important role in prevention of the pathological process of DR. Two experiments were performed. gCTRP3 or vehicle was administered via peritoneal implant osmotic pumps for 2 weeks to HFD/STZ mice and the age-matched nondiabetic mice. Concentrations of gCTRP3 in serum and retina were decreased in diabetic mice compared to control. Administered of gCTRP3 (0.5 μg/g/d) replenished gCTRP3 level (sFig. 3A,3C and 3D). As capillary leakage is a golden standard reflecting microvascular damage [24], we first performed the Miles permeability assay to identify gCTRP3 protective effect. Although administration of gCTRP3 had no significant effect on body weight, blood glucose levels and insulin sensitivity (Fig. 1C-1F), it markedly prevented extravasation of Evans blue dye (Fig. 1A and 1B). Therefore, these data suggest that gCTRP3 treatment significantly preserved the capillary barrier function in the T2D model. Second, to further illustrate the effect of CTRP3 specifically on retinal vascular permeability, we evaluated retina vascular extravasation after administered CTRP3 to animals with diabetic retinopathy. As illustrated in Fig. 2A and 2C, retina vascular extravasation (green color) was obviously increased in T2D model. However, it was markedly decreased after CTRP3 administered, suggesting that CTRP3 effectively reduced retinal capillary leakage. In addition, no neovascularization were observed, indicating that gCTRP3 did not significantly promote angiogenesis (Fig. 2A and 2B).

CTRP3 protected barrier function of inner blood-retinal barrier (iBRB) against HGHL-induced impairment

Retinal neovascularization is a severe complication in diabetic retinal pathology. To directly investigate whether CTRP3 has the effect on angiogenesis in the early stage of diabetes, we determined the effect of CTRP3 upon tube formation in cultured HRMECs. HRMECs cultured in NGNL or HGHL medium for 24 hours with vehicle or gCTRP3 pre-treatment. CTRP3 had no significant effect on tube formation (Fig. 3A ad 3B). Since the inner blood-retinal barrier (iBRB) is a structure of tight junctions among HRMECs, preventing retinal capillary leakage, we performed 3 serial experiments to further clarify whether CTRP3 could protect integrity and function of iBRB. First, we utilized in-vitro xCELLigence electrical conductivity assays to evaluate the cell-cell junctions of the iBRB. Cell index curve rose sharply and then stabilized, which suggested that iBRB was formed and functional (SFig. 2A). As illustrated as Fig. 3C, gCTRP3 addition alone did not affect the permeability of the iBRB. However, when CTRP3 was added to HRMECs followed by HGHL administration, iBRB permeability was successfully prevented by gCTRP3 treatment (Fig. 3C to 3D). Second, we performed an in-vitro endothelial transwell permeability assay. HRMECs monolayer (iBRB) permeability was determined by measuring FITC-dextran signal (iBRB permeability indicator) on the endothelial monolayer as indicated in sFig. 2B. The iBRB permeability was significantly increased when challenged with HGHL, whereas the HGHL-induced increase was successfully blocked by gCTRP3 pre-treatment (Fig. 3E). Thirdly, we performed immuno-fluorescence staining for tight junctions

with Occludin and Claudin-5 in HRMECs to determine whether gCTRP3 can protect integrity of iBRB from HGHL-induced damage. HGHL treatment disrupted endothelial cell-to-cell junctions. This disruption of junctions was effectively prevented by gCTRP3 pre-treatment (Fig. 3F to 3H). These results suggested that gCTRP3 maintained barrier function of iBRB, preventing HGHL-induced permeability.

CTRP3 increased Occludin and Claudin-5 expression and protected iBRB from HGHL-induced impairment

To identify the molecular mechanisms underlying the effects of CTRP3 on the iBRB protection, we screened the expression of iBRB related tight junction proteins including Claudin-1, Zonula occludens-1 (ZO-1), Claudin-5, Occludin in HRMECs. As indicated in Fig. 4A-4E, pre-treatment with gCTRP3 increased Occludin and Claudin-5 expression in a dose dependent manner and successfully prevented the HGHL-induced suppression of Occludin and Claudin-5 level. gCTRP3 alone did not cause alteration of tight junction protein expression. Taken together, these results provide clear evidence that gCTRP3 increased Occludin and Claudin-5 expression and protected the integrity of iBRB from HGHL-induced damage.

CTRP3 increased Occludin and Claudin-5 (tight junction protein) expression in HRMECs via AMPK activation in vitro

Next, we screened metabolism and survival related signaling pathways to determine the upstream signaling molecules mediating the expression of Occludin and Claudin-5. Although several studies have reported AMPK signal was suppressed in diabetes,[25] whether the protective role of CTRP3 on iBRB's tight junction observed here in this study are associated with AMPK is unclear. CTRP3 treatment significantly increased AMPK phosphorylation. However, Akt was not significantly activated by CTRP3 in HRMECs (Fig. 5A and 5B). In addition, with AMPK silenced HRMECs followed by gCTRP3 pre-treatment (3μg/ml, 15 minutes) and HGHL administration, we identified that gCTRP3 failed to block the HGHL-induced decrease of Claudin-5 and Occludin expression (Fig. 5C and 5D), suggesting that AMPK activation is required for gCTRP3's regulation in Occludin and Claudin-5 expression. Meanwhile, the activation of acetyl-CoA carboxylase (AMPK's direct target) was evaluated. CTRP3 successfully restored HGHL inhibited-ACC phosphorylation (Fig. 5C and 5D). In order to determine AMPK's role in CTRP3's influence on cell-to-cell junctions of iBRB, we utilized xCELLigence electrical conductivity assay. AMPK silence effectively blocked the protective effect of gCTRP3 on HGHL-induced iBRB disruption (Fig. 5E and 5F). Taken together, these results provided clear evidence that CTRP3 increased Occludin and Claudin-5 tight junctions protein expression and exerts its iBRB- protection effect via AMPK-dependent signaling.

CTRP3-induced increase of Occludin and Claudin-5 are abolished after inhibition of AMPK in vivo

To confirm whether CTRP3 protects iBRB's tight junction via AMPK signaling in vivo, 10 mg/kg Compound C (an AMPK inhibitor) was intraperitoneally injected into diabetic mice daily for 2 weeks. We then assessed pAMPK, AMPK, pACC, ACC, ZO-1, Occludin, Claudin-1 and Claudin-5 expression in each group. Consistent with in vitro data, DR inhibited AMPK and ACC activity and Occludin, Claudin-5 expression. Administration of gCTRP3 reversed those changes in the retinal tissue in DR model. However, these effects were blocked by Compound C administration (Fig. 6A-6C). These results suggest that

CTRP3 maintained the barrier function of iBRB in DR by preventing the diabetes-induced Occludin and Claudin-5/tight junctions protein disruption via AMPK-dependent signaling.

Discussion

In the current study, we report that CTRP3 preserves iBRB function in NPDR through preventing diabetic suppression of Occludin and Claudin-5 (tight junction protein) expression in an AMPK dependent manner. This study suggests that CTRP3 may have therapeutic potential to the diabetic retina by decreasing vascular permeability, and preventing CTRP3 reduction is a promising therapeutic approach during the management of DR.

Despite years of ongoing scientific investigation, the fundamental phenotypic properties governing the increased incidence of diabetes and its complications, especially in DR, remain largely unknown. DR development involves two stages, NPDR and PDR. iBRB injury has been implicated in the initiation and progress of retina complications of diabetes, particularly during NPDR. Plasma leakage and fluid retention are seen in various tissues of diabetic patients or animals at the early stages of the disease (NPDR) before structural microangiopathy can be detected (PDR). CTRP3, as the important regulatory factor of adipose-derived hormones and cytokines (adipokines and adiponectin paralogs) in diabetes, has gained recognition [8] [26, 27]. We have recently demonstrated that circulating CTRP3 may serve as a valuable biomarker screening diabetic retinopathy in patients as it is inversely associated with DR severity [12]. Diabetes is a group of metabolic diseases characterized by hyperglycemia resulting from defects in insulin action. However, in this study we demonstrated that CTRP3 did not present the metabolic regulatory effect on type 2 diabetes while it prohibited capillary vascular leakage in the late stage of diabetic model. CTRP3 may therefore have clinical application to NPDR, a pathology requiring advancements in treatment options. CTRP3 has been reported to exert anti-apoptotic effects [28], and attenuate diabetes-related injuries [29, 30] including the inflammatory processes of DR [19], suggesting the therapeutic potential of CTRP3 for the treatment of DR. To test this hypothesis, we utilized globular domain isoform of CTRP3 (gCTRP3) to investigate its effect on early stage of diabetic retinopathy (NPDR). gCTRP3 can be generated via proteolytic cleavage of full-length CTRP3 (fCTRP3) with functions as the active isoform [31]. Although retinal neovascularization is a severe complication in DR, in this study, we focus on CTRP3's effect on early stage of diabetic DR (NPDR) when the neovascularization did not obviously occur, but CTRP3 can ameliorate the leakage of iBRB as manifested in Fig. 2A and 2B with FITC-Dextran tracing. In addition, we demonstrated retinal neovascularization was not observed with TRITC-ConcanavalinA tracing. Meanwhile, tube formation experiment demonstrated that CTRP3 did not directly increase angiogenesis on cellular level. Therefore, we have confirmed that CTRP3 did not affect retinal angiogenesis in vivo and in vitro, but preventing the permeability of iBRB.

Next, we demonstrated that CTRP3 significantly reduced not only capillaries leakage of retina but also capillaries leakage on micro grade vessels in vivo. Specifically, we have observed that extravasation of Evans blue dye is significantly increased in DR mice, a pathologic alteration markedly inhibited by CTRP3.

These results indicate that CTRP3 treatment protects barrier integrity and preserves junctions of capillary from diabetes induced injury

Retinal neovascularization is a severe complication in DR. The effect of CTRP3 upon angiogenesis remains controversial [32] [33]. TRITC-ConcanavalinA/FITC-dextran permeability assay that we utilized in the study is a method to present vascular structures with high resolution and can provide solid evidence on retinal capillary permeability and angiogenesis in retina. However, based on the results from in vivo retinal vascularity examination, we observed that CTRP3 had no significant effect on retinal neovascularization in this early stage of diabetic DR model (NPDR). It is worth noting that in our pilot experiments, CTRP3 failed to exert significant protective effect in diabetes-induced severe DR mice model (PDR model) (18 weeks after diabetes onset), suggesting that early treatment with CTRP3 is crucial.

Third, we report the protective effect of CTRP3 against HGHL-induced inner blood-retinal barrier (iBRB) impairment. iBRB, as a key barrier in developing novel therapeutics for DR, contains tight-junctions (TJ's) among adjacent endothelial cells lining the fine capillaries of the retinal [34, 35]. TJs are comprised of membrane spanning proteins (Claudins, Occludin and Junctional adhesion molecules) which interact with cytoplasmic proteins (ZO-1) [36, 37]. gCTRP3 did not affect iBRB under normal circumstances. However, CTRP3 preserves Occludin and Claudin-5 level in diabetic HRMECs. Furthermore, consistent with previous clinical studies[38, 39], we report that CTRP3 significantly increased AMPK phosphorylation, the mechanism through which CTRP3 effectively regulates the levels of Occludin and Claudin-5 in iBRB. These in vitro results were confirmed in vivo DR model by analysis of tight junction's protein in the retinal tissue. It should be indicated that although multiple AMPK activators, such as metformin, are current available, CTRP3 has its clear advantage. CTRP3 does not influence animal weight, blood glucose level and OGTT. Therefore, CTRP3's protective effect against diabetic DR process is independent of glucose's regulation. More importantly, metformin is a chemical AMPK activator. Its dose must be precisely titrated to achieve optimal AMPK activation as overactivation of AMPK may have adverse effect. In contrast, CTRP3 is an endogenous molecule with AMPK activation capability. A replacement strategy to restore CTRP3 back to its normal level in diabetic model (as utilized in the current study) is more desirable.

There are several limitations in the current study. First, we used HFD/STZ-induced T2D model. Whether CTRP3 may also protect in a genetic T2D model remains unknown [40, 41]. Second, cell type and stimuli conditions may be responsible for the variant effects we observed when compared with other endothelial cell related studies. In addition, we recognize that the pathophysiology of DR is highly complex and multifactorial. It involves the activation of several interrelated pathways, including increased oxidative stress, increased pro-inflammatory mediators and induced VEGF secretion. These pathologic alterations all occur on a background of the various metabolic derangements that are inherent to DM [42] and there are more to learn in this complex interactions. Some questions remain unanswered and need to be further explored. These include how AMPK signals regulates Occludin and Claudin-5 expression, and whether AMPK regulate their phosphorylation and/or intracellular translocation.

Conclusion

Our results identify CTRP3 as a prominent adipokine, exerting the iBRB- protection through upregulating Occludin and Claudin-5 in DR in an AMPK-dependent manner. Thus, CTRP3 may serve as not only a biomarker as we previously reported (reference) but also a promising preventive and therapeutic mean for DR and associated complications of T2D.

Abbreviations

iBRB
inner blood-retinal barrier
DR
Diabetic retinopathy
gCTRP3
globular C1q/tumor necrosis factor-related proteins-3
NPDR
non-proliferative diabetic retinopathy
HG/HL
high glucose/high lipids
HRMECs
human retinal endothelial cells
T2D
Type 2 diabetes
STZ
Streptozotocin

Declarations

Ethics approval and consent to participate

Not applicable.

Consent for publication

Not applicable.

Availability of data and materials

All data generated or analyzed during this study are included in this published article

Competing interests

The authors declare that they have no competing interests.

Funding

Financial support for these studies was provided by American Diabetes Association (1-17-IBS-297); W.W. Smith Charitable Trust (H1702); National Institutes of Health (HL-96686, X. Ma/Y. Wang, MPI; HL-123404, X. Ma).

Acknowledgments. The authors thank Professor Ulhas P. Naik (Thomas Jefferson University) for xCELLigence analysis.

Author Contributions

Y. W. and X. M. was involved in experimental design, experiments, data analysis and interpretation. Z.Y., C.W., L.G., R.G., J.L., Z.M. and J.Z. performed experiments and Y.Z. X.J., and J.C. collected the analyzed data. Z.Y. wrote the manuscript. W.L., B.L., U.N., Z.W., and T.C. were involved in data analysis and interpretation. All authors approved the final version of the manuscript.

References

1. Solomon SD, Chew E, Duh EJ, Sobrin L, Sun JK, VanderBeek BL, Wykoff CC, Gardner TW. Diabetic retinopathy: a position statement by the American Diabetes Association. Diabetes Care. 2017;40(3):412–8.
2. Das A, McGuire PG, Rangasamy S. Diabetic macular edema: pathophysiology and novel therapeutic targets. Ophthalmology. 2015;122(7):1375–94.
3. Qaum T, Xu Q, Joussen AM, Clemens MW, Qin W, Miyamoto K, Hassessian H, Wiegand SJ, Rudge J, Yancopoulos GD. VEGF-initiated blood–retinal barrier breakdown in early diabetes. Investig Ophthalmol Vis Sci. 2001;42(10):2408–13.
4. El-Remessy AB, Behzadian MA, Abou-Mohamed G, Franklin T, Caldwell RW, Caldwell RB. Experimental diabetes causes breakdown of the blood-retina barrier by a mechanism involving tyrosine nitration and increases in expression of vascular endothelial growth factor and urokinase plasminogen activator receptor. Am J Pathol. 2003;162(6):1995–2004.
5. Li J, Wang P, Ying J, Chen Z, Yu S. Curcumin attenuates retinal vascular leakage by inhibiting calcium/calmodulin-dependent protein kinase II activity in streptozotocin-induced diabetes. Cell Physiol Biochem. 2016;39(3):1196–208.
6. Joussen AM, Murata T, Tsujikawa A, Kirchhof B, Bursell S-E, Adamis AP. Leukocyte-mediated endothelial cell injury and death in the diabetic retina. Am J Pathol. 2001;158(1):147–52.
7. Zhang SX, Ma J-x, Sima J, Chen Y, Hu MS, Ottlecz A, Lambrou GN. Genetic difference in susceptibility to the blood-retina barrier breakdown in diabetes and oxygen-induced retinopathy. Am J Pathol. 2005;166(1):313–21.
8. Ouchi N, Walsh K. **Cardiovascular and metabolic regulation by the adiponectin/CTRP family of proteins**. In.: Am Heart Assoc; 2012.
9. Kopp A, Bala M, Buechler C, Falk W, Gross P, Neumeier M, Scholmerich J, Schaffler A. C1q/TNF-related protein-3 represents a novel and endogenous lipopolysaccharide antagonist of the adipose

tissue. Endocrinology. 2010;151(11):5267–78.

10. Hofmann C, Chen N, Obermeier F, Paul G, Büchler C, Kopp A, Falk W, Schäffler A. C1q/TNF-related protein-3 (CTRP-3) is secreted by visceral adipose tissue and exerts antiinflammatory and antifibrotic effects in primary human colonic fibroblasts. Inflamm Bowel Dis. 2011;17(12):2462–71.
11. Ban B, Bai B, Zhang M, Hu J, Ramanjaneya M, Tan BK, Chen J. Low serum cartonectin/CTRP3 concentrations in newly diagnosed type 2 diabetes mellitus: in vivo regulation of cartonectin by glucose. PloS one. 2014;9(11):e112931.
12. Yan Z, Zhao J, Gan L, Zhang Y, Guo R, Cao X, Lau WB, Ma X, Wang Y. CTRP3 is a novel biomarker for diabetic retinopathy and inhibits HGHL-induced VCAM-1 expression in an AMPK-dependent manner. PloS one. 2017;12(6):e0178253.
13. Akiyama H, Furukawa S, Wakisaka S, Maeda T. CTRP3/cartducin promotes proliferation and migration of endothelial cells. Molecular cellular biochemistry. 2007;304(1–2):243.
14. Shao M, Lu X, Cong W, Xing X, Tan Y, Li Y, Li X, Jin L, Wang X, Dong J. **Multiple low-dose radiation prevents type 2 diabetes-induced renal damage through attenuation of dyslipidemia and insulin resistance and subsequent renal inflammation and oxidative stress**. *PloS one* 2014, 9(3).
15. Lee C-S, Kim YG, Cho H-J, Park J, Jeong H, Lee S-E, Lee S-P, Kang H-J, Kim H-S. Dipeptidyl peptidase-4 inhibitor increases vascular leakage in retina through VE-cadherin phosphorylation. Scientific reports. 2016;6(1):1–16.
16. Xie H, Zhang C, Liu D, Yang Q, Tang L, Wang T, Tian H, Lu L, Xu JY, Gao F, et al. Erythropoietin protects the inner blood-retinal barrier by inhibiting microglia phagocytosis via Src/Akt/cofilin signalling in experimental diabetic retinopathy. Diabetologia. 2021;64(1):211–25.
17. Tagami M, Kusuhara S, Honda S, Tsukahara Y, Negi A. Expression of ATP-binding cassette transporters at the inner blood-retinal barrier in a neonatal mouse model of oxygen-induced retinopathy. Brain Res. 2009;1283:186–93.
18. Li H, Mei XY, Wang MN, Zhang TY, Zhang Y, Lu B, Sheng YC. Scutellarein alleviates the dysfunction of inner blood-retinal-barrier initiated by hyperglycemia-stimulated microglia cells. Int J Ophthalmol. 2020;13(10):1538–45.
19. Liu G-Z, Liang B, Lau WB, Wang Y, Zhao J, Li R, Wang X, Yuan Y, Lopez BL, Christopher TA. High glucose/High Lipids impair vascular adiponectin function via inhibition of caveolin-1/AdipoR1 signalsome formation. Free Radic Biol Med. 2015;89:473–85.
20. Capozzi ME, Giblin MJ, Penn JS. Palmitic Acid Induces Muller Cell Inflammation that is Potentiated by Co-treatment with Glucose. Sci Rep. 2018;8(1):5459.
21. Adil MS, Somanath PR: **Endothelial Permeability Assays In Vitro**. 2020.
22. Chen H-R, Yeh T-M: **In vitro Assays for Measuring Endothelial Permeability by Transwells and Electrical Impedance Systems**. 2017.
23. Schwarz M, Jendrusch M, Constantinou I. Spatially resolved electrical impedance methods for cell and particle characterization. Electrophoresis. 2020;41(1–2):65–80.

24. Lee C-S, Kim YG, Cho H-J, Park J, Jeong H, Lee S-E, Lee S-P, Kang H-J, Kim H-S. Dipeptidyl peptidase-4 inhibitor increases vascular leakage in retina through VE-cadherin phosphorylation. Scientific reports. 2016;6:29393.
25. Jeon SM. Regulation and function of AMPK in physiology and diseases. Exp Mol Med. 2016;48(7):e245.
26. Peterson JM, Wei Z, Wong GW. **C1q/TNF-related protein-3 (CTRP3): a novel adipokine that regulates hepatic glucose output**. *Journal of Biological Chemistry* 2010:jbc. M110. 180695.
27. Kopp A, Bala M, Weigert J, Büchler C, Neumeier M, Aslanidis C, Schölmerich J, Schäffler A. Effects of the new adiponectin paralogous protein CTRP-3 and of LPS on cytokine release from monocytes of patients with type 2 diabetes mellitus. Cytokine. 2010;49(1):51–7.
28. Mu Y, Yin T-l, Yin L, Hu X, Yang J. **CTRP3 attenuates high-fat diet-induced male reproductive dysfunction in mice**. *Clinical Science* 2018:CS20180179.
29. Choi KM, Hwang SY, Hong HC, Yang SJ, Choi HY, Yoo HJ, Lee KW, Nam MS, Park YS, Woo JT. **C1q/TNF-related protein-3 (CTRP-3) and pigment epithelium-derived factor (PEDF) concentrations in patients with type 2 diabetes and metabolic syndrome**. *Diabetes* 2012:DB_120217.
30. Choi HY, Park JW, Lee N, Hwang SY, Cho GJ, Hong HC, Yoo HJ, Hwang TG, Kim SM, Baik SH. **Effects of a combined aerobic and resistance exercise program on C1q/TNF-related protein-3 (CTRP-3) and CTRP-5 levels**. *Diabetes Care* 2013:DC_130178.
31. Yi W, Sun Y, Yuan Y, Lau WB, Zheng Q, Wang X, Wang Y, Shang X, Gao E, Koch WJ: **C1q/TNF-related protein-3, a newly identified adipokine, is a novel anti-apoptotic, pro-angiogenic, and cardioprotective molecule in the ischemic mouse heart**. *Circulation* 2012:CIRCULATIONAHA. 112.099937.
32. Seldin MM, Tan SY, Wong GW. Metabolic function of the CTRP family of hormones. Reviews in Endocrine Metabolic Disorders. 2014;15(2):111–23.
33. Ma X-L: **C1q/TNF-Related Protein-3, a Newly Identified Adipokine, is a Novel Anti-Apoptotic, Pro-Angiogenic, and Cardioprotective Molecule in the Ischemic Mouse Heart**. 2011.
34. Kady NM, Liu X, Lydic TA, Syed MH, Navitskaya S, Wang Q, Hammer SS, O'Reilly S, Huang C, Seregin SS. **ELOVL4-Mediated Production of Very Long Chain Ceramides Stabilizes Tight Junctions and Prevents Diabetes-Induced Retinal Vascular Permeability**. *Diabetes* 2018:db171034.
35. Campbell M, Nguyen ATH, Kiang A-S, Tam L, Kenna PF, Dhubhghaill SN, Humphries M, Farrar GJ, Humphries P: **Reversible and size-selective opening of the inner blood-retina barrier: a novel therapeutic strategy**. In: *Retinal Degenerative Diseases.* Springer; 2010: 301–308.
36. Shen W, Li S, Chung SH, Zhu L, Stayt J, Su T, Couraud P-O, Romero IA, Weksler B, Gillies MC. Tyrosine phosphorylation of VE-cadherin and claudin-5 is associated with TGF-β1-induced permeability of centrally derived vascular endothelium. Eur J Cell Biol. 2011;90(4):323–32.
37. Luo Y, Xiao W, Zhu X, Mao Y, Liu X, Chen X, Huang J, Tang S, Rizzolo LJ. Differential expression of claudins in retinas during normal development and the angiogenesis of oxygen-induced retinopathy. Investig Ophthalmol Vis Sci. 2011;52(10):7556–64.

38. Kim J-Y, Min J-Y, Baek JM, Ahn S-J, Jun HY, Yoon K-H, Choi MK, Lee MS, Oh J. CTRP3 acts as a negative regulator of osteoclastogenesis through AMPK-c-Fos-NFATc1 signaling in vitro and RANKL-induced calvarial bone destruction in vivo. Bone. 2015;79:242–51.
39. Zhang C-L, Feng H, Li L, Wang J-Y, Wu D, Hao Y-T, Wang Z, Zhang Y, Wu L-L. Globular CTRP3 promotes mitochondrial biogenesis in cardiomyocytes through AMPK/PGC-1α pathway. Biochimica et Biophysica Acta (BBA)-General Subjects. 2017;1861(1):3085–94.
40. Wang H, Shi H, Zhang J, Wang G, Zhang J, Jiang F, Xiao Q: **Toll-like receptor 4 in bone marrow-derived cells contributes to the progression of diabetic retinopathy**. *Mediators of inflammation* 2014, **2014**.
41. Villacampa P, Ribera A, Motas S, Ramírez L, García M, de la Villa P, Haurigot V, Bosch F. **Insulin-like growth factor I (IGF-I)-induced chronic gliosis and retinal stress lead to neurodegeneration in a mouse model of retinopathy**. *Journal of Biological Chemistry* 2013:jbc. M113. 468819.
42. Pusparajah P, Lee L-H, Abdul Kadir K. Molecular markers of diabetic retinopathy: potential screening tool of the future? Frontiers in physiology. 2016;7:200.

Figures

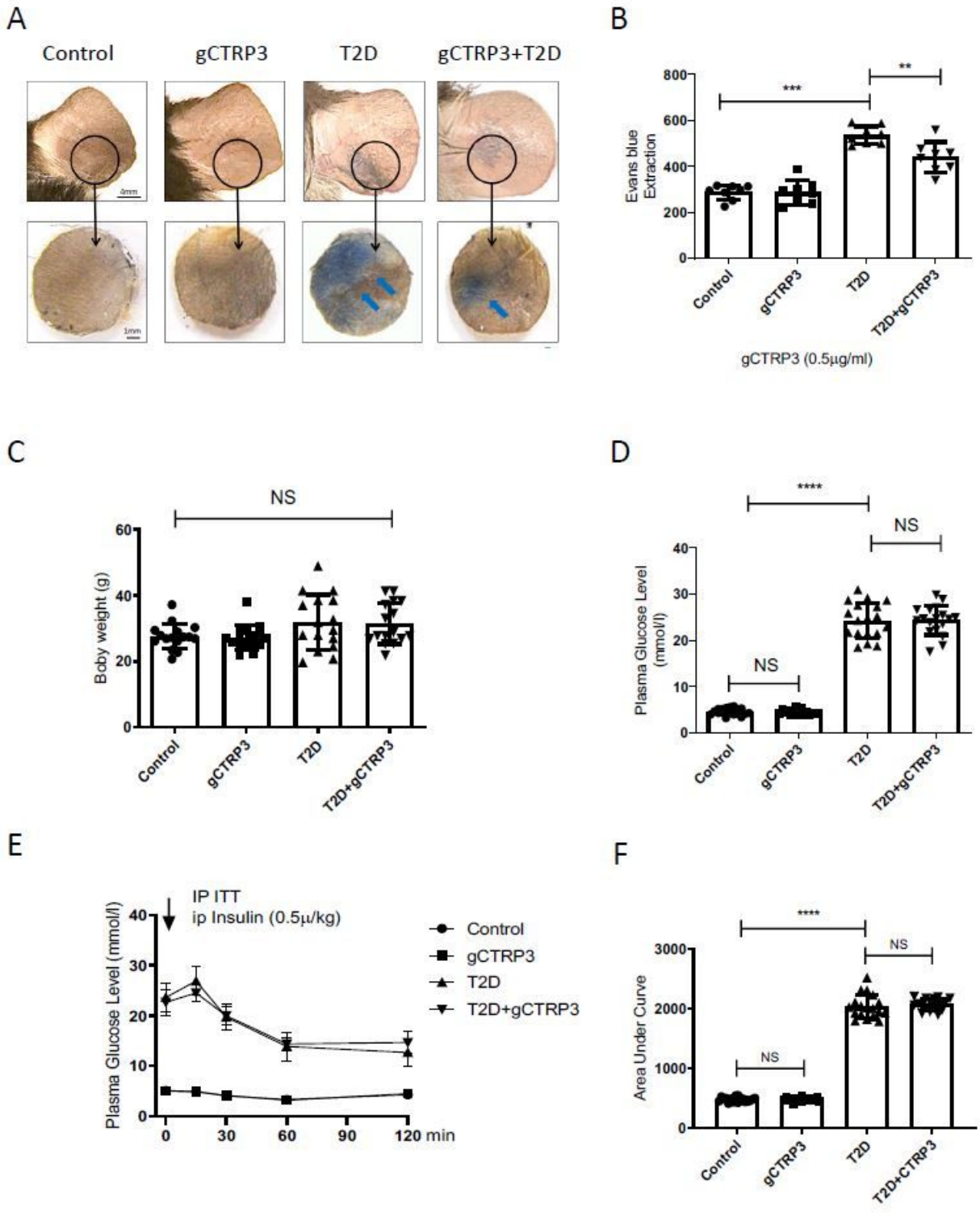

Figure 1

gCTRP3 ameliorated T2D-induced capillary leakage A, Representative images showing that gCTRP3 (0.5μg/g/d) reduced evens blue dye leakage to dermal adjacent tissue in T2D mice. B, Quantification with column graph analysis (n=8-10). C, gCTRP3 failed to affect body weight, blood glucose levels (D) and insulin resistance (E,F) in diabetic retinopathy group compared with Sham. All data are shown as means

± SD. n = 18 for each group. **P <0.01, ***P <0.001; NS, no significance. Blue arrows indicate ear capillary leakage. HFD, high fat diet. ND, normal diet.

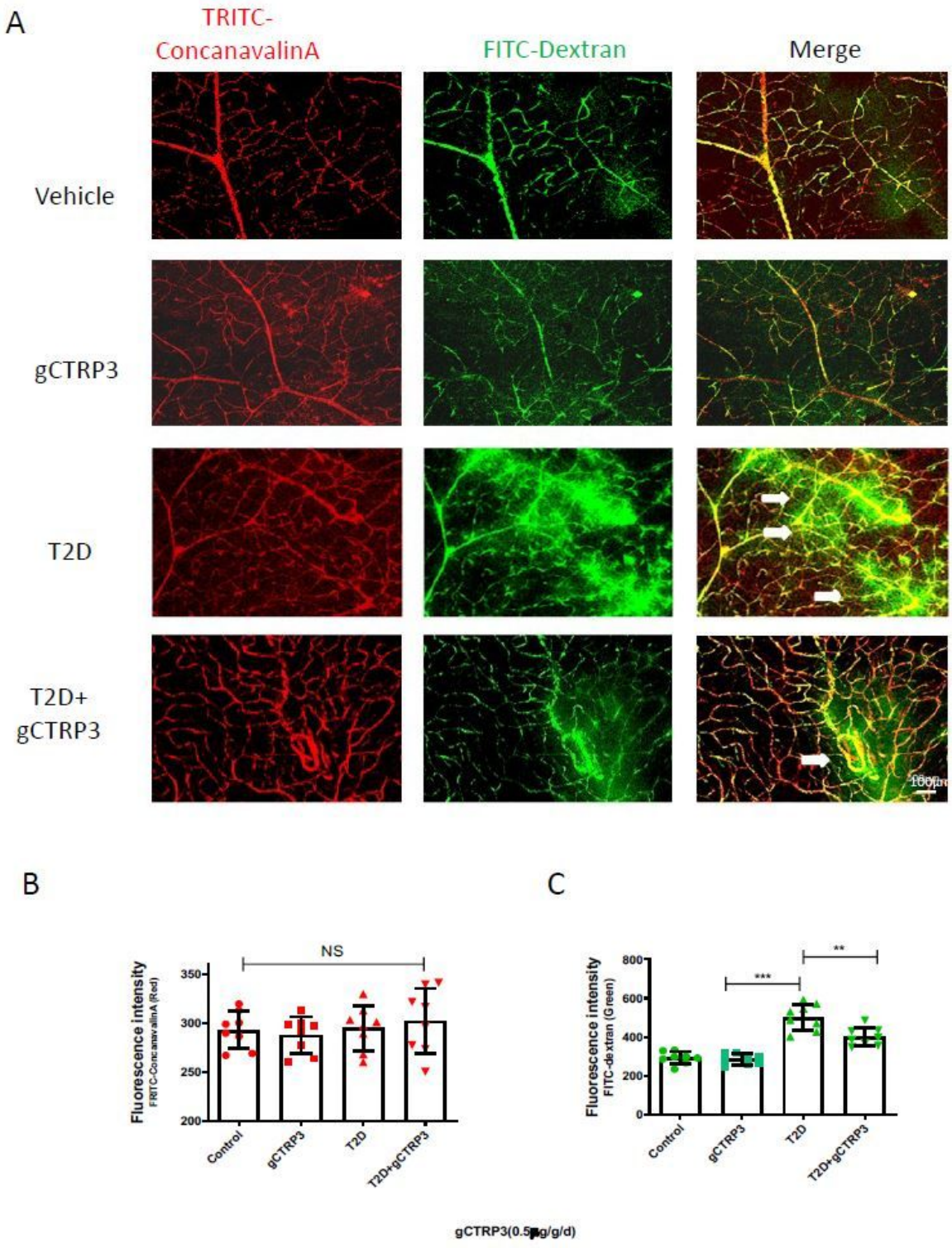

Figure 2

The protective effect of CTRP3 on DR A, Representative images showing that CTRP3 reduced the retinal vascular leakage which was increased in the T2D DR group. B, Representative images showing that no visible neovascularization evaluated with TRITC-ConcanavalinA signal (intact retinal vessels, red). C,

Significant extravasation of FITC-dextran (vascular leakage, green) was observed in T2D-DR mice, but it was reduced by CTRP3. All data are shown as means ± SD. n = 8-10 for each group. **P < 0.01, ***P < 0.001; NS, not significant. White arrows indicate retinal vascular leakage. T2D, Type 2 diabetes. DR, Diabetic retinopathy.

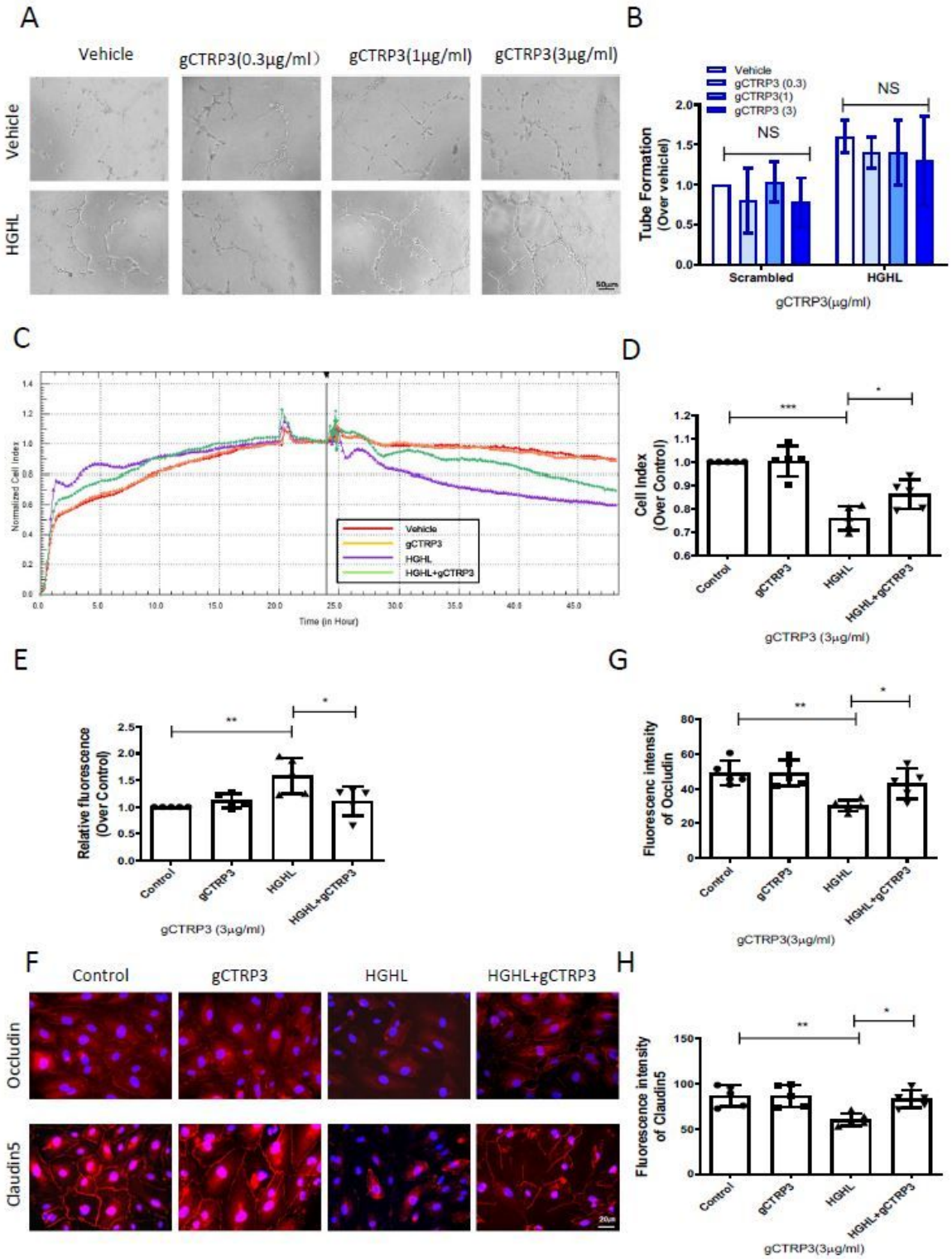

Figure 3

gCTRP3 protected barrier function of iBRB against HGHL-induced damage A, Representative images for tube formation assay showing that gCTRP3 failed to promote HREMCs tube formation. B, Bar graph for tube formation analysis, n = 5. C, Representative images for xCELLigence electrical conductivity assays showing that gCTRP3 increased cellular connection. D, Bar graph analysis for xCELLigence conductivity assay. E, Bar graph analysis for Transwell endothelial permeability assay. F, Immunoflurencence images showing that HGHL disrupted cell-to-cell junctions in HRMECs staining with Occludin (red), Claudin-5 (red), Nuclei (blue). G, H, Fluorescence intensity quantification of Occludin (red), Claudin-5. HRMECs were treated with vehicle or HGHL for 24 hours followed by CTRP3 administration (3μg/ml). All data are shown as means ± SD. n = 5 for each group. Bar graph represent analysis from at least 5 independent repeated experiments. *P < 0.05, **P < 0.01, ***P < 0.001. HGHL, high glucose and high lipids.

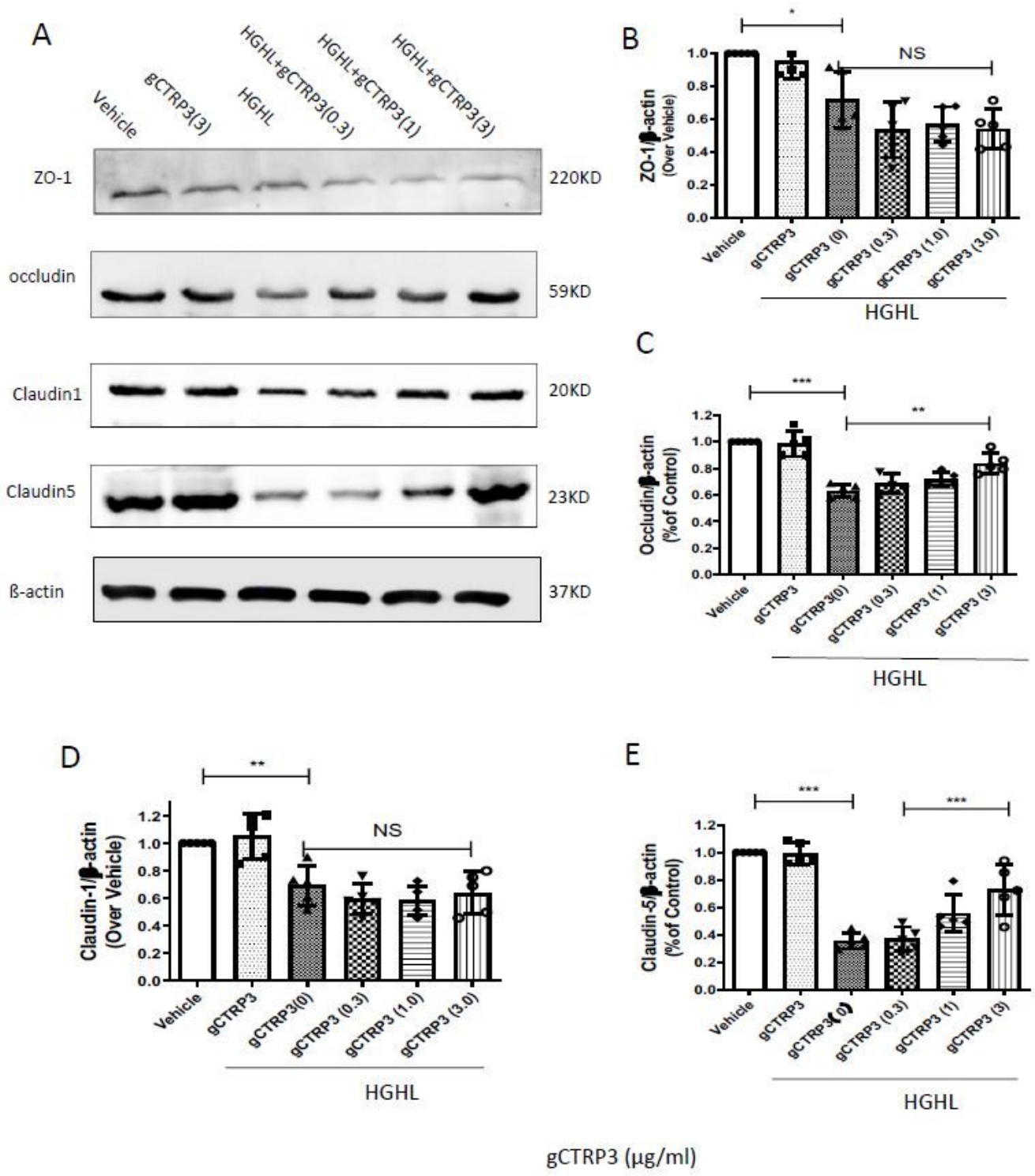

Figure 4

CTRP3 increased Occludin and Claudin-5 expression and protected integrity of iBRB against HGHL-induced damage A, Representative immunoblots showing that Claudin-1, ZO -1, Claudin-5 and Occludin protein levels in HRMECs pre-treated with gCTRP3 (3μg/ml) followed by HGHL administration. B, Bar graph analysis for quantification of ZO-1 protein expression. C, Bar graph analysis for quantification of Occludin protein expression. D, Bar graph analysis for quantification of Claudin1 protein expression. E,

Bar graph analysis for quantification of Claudin5 protein expression. All data are shown as means ± SD. n=5-7. Bar graph represent analysis from at least 5 independent repeated experiments. *P < 0.05, **P < 0.01. ***P < 0.001; NS, No significance.

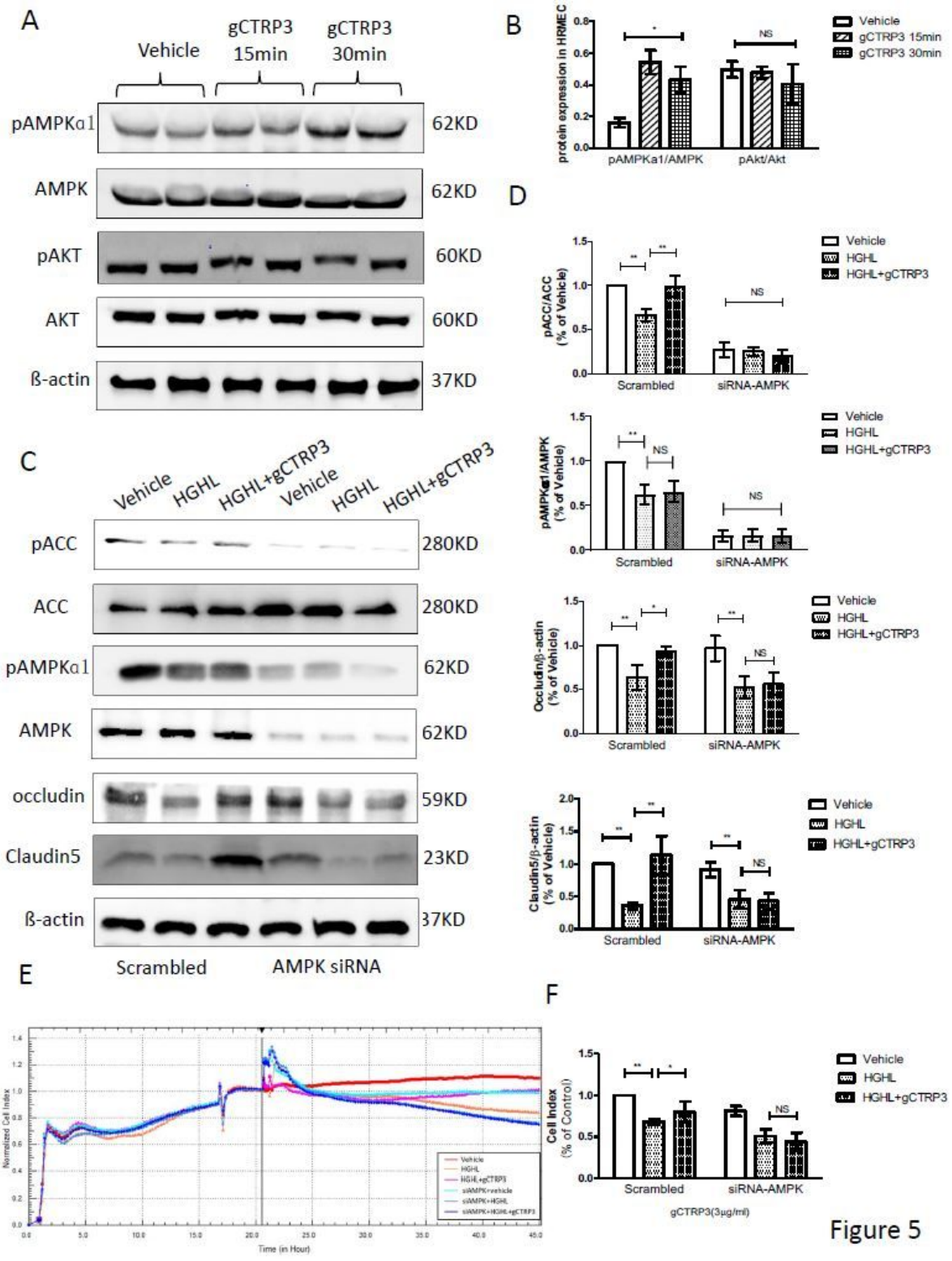

Figure 5

Figure 5

Inhibition of AMPK blocked CTRP3's role in upregulation of Occludin and Claudin 5 A, Representative immunoblots showing that AMPK and Akt activation in HREMCs treated with gCTRP3. B, The bar graph

showing the quantification of AMPK and Akt activation. HRMECs were challenged by gCTRP3 (3 μg/ml) for 15 minutes followed by HGHL administration (n=5-7). C, Western blot analysis confirmed successful knockdown of AMPK by siRNA and expression of pAMPK, AMPK, pACC, ACC, Occludin and Claudin-5. D, Bar graph for quantification of the level of key molecules.. E, xCELLigence electrical conductivity assays showed the role of AMPK in HREMCs pretreated with CTRP3 followed by HGHL challenge. F, Bar graph for analysis of xCELLigence electrical conductivity assay. n = 5-7. Bar graph represent analysis from at least 5 independent repeated experiments. All data are shown as means ± SD. *P < 0.05, **P < 0.01; NS, no significance. HGHL, high glucose and high lipids.

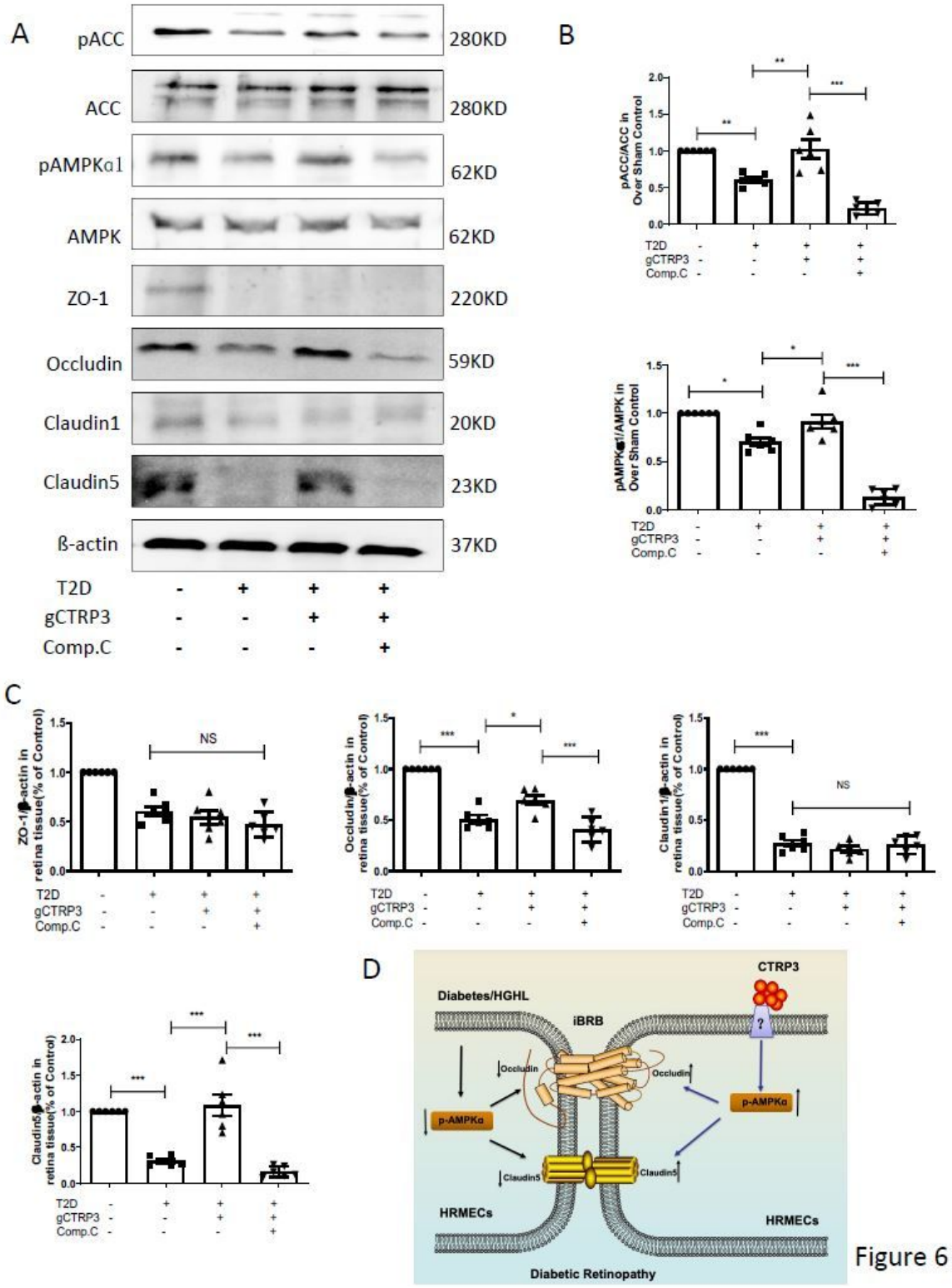

Figure 6

Figure 6

AMPK deficiency blocked CTRP3 upregulated the protein level of Occludin, Claudin-5 in DR A: Representative Western blots of pAMPK, AMPK, pACC, ACC, Claudin-1, ZO-1, Claudin-5 and Occludin in retina from Sham and T2D/STZ DR mice with/without gCTRP3 treatment and Compound C administration. B, Bar graph for quantification of the expression of pAMPK, AMPK, pACC, ACC. C, Bar graph for quantification of the expression of Claudin-1, ZO-1, Claudin-5 and Occludin. D, Diagram depicts

mechanism responsible for the iBRB protective effects of CTRP3 on diabetic retinopathy. n = 6-8. Bar graph represent analysis from at least 6 independent repeated experiments. All data are shown as means ± SD. *P < 0.05, **P < 0.01. ***P < 0.001; NS, no significance. DR, diabetic retinopathy. T2D, type 2 diabetes. Comp. C, Compound C.

Supplementary Files

This is a list of supplementary files associated with this preprint. Click to download.

- SupplementFigures.pdf
- Unmodifiedgel.pdf